JOURNAL OF NEUROTRAUMA 35:780–789 (March 1, 2018)
© Mary Ann Liebert, Inc.
DOI: 10.1089/neu.2017.5362

A Novel Method for Quantifying Human *In Situ* Whole Brain Deformation under Rotational Loading Using Sonomicrometry

Ahmed Alshareef, J. Sebastian Giudice, Jason Forman, Robert S. Salzar, and Matthew B. Panzer

Downloaded by Univ Of Western Ontario from www.liebertpub.com at 04/11/18. For personal use only.

Abstract

Traumatic brain injuries (TBI) are one of the least understood injuries to the body. Finite element (FE) models of the brain have been crucial for understanding concussion and for developing injury mitigation systems; however, the experimental brain deformation data currently used to validate these models are limited. The objective of this study was to develop a methodology for the investigation of *in situ* three-dimensional brain deformation during pure rotational loading of the head, using sonomicrometry. Sonomicrometry uses ultrasonic pulses to measure the dynamic distances between piezoelectric crystals implanted in any sound-transmitting media. A human cadaveric head-neck specimen was acquired 14 h postmortem and was instrumented with an array of 32 small sonomicrometry crystals embedded in the head: 24 crystals were implanted in the brain, and 8 were fixed to the inner skull. A dynamic rotation was then applied to the head using a closed-loop controlled test device. Four pulses with different severity levels were applied around three orthogonal anatomical axes of rotation. A repeated test of the highest severity rotation was conducted in each axis to assess repeatability. All tests were completed within 56 h postmortem. Overall, the combined experimental and sonomicrometry methods were demonstrated to reliably and repeatedly capture three-dimensional dynamic deformation of an intact human brain. These methods provide a framework for using sonomicrometry to acquire multidimensional experimental data required for FE model development and validation, and will lend insight into the deformations sustained by the brain during impact.

Keywords: brain deformation; FE validation; sonomicrometry; TBI

Introduction

Traumatic brain injuries (TBI) are one of the most common but least understood injuries to the body. It is estimated that 1,700,000 TBIs occur in the United States annually from impacts during competitive sports, motor vehicle crashes, and falls.[1] Various mechanisms for TBI have been studied for decades in an attempt to link external head kinematics (linear and rotational motion) to the macroscopic and microscopic deformations of brain tissue that leads to injury. The focus on correlating external head kinematics to brain injury risk has been motivated in part by the goal of developing TBI risk functions for assessing the efficacy of helmets and automotive countermeasures.[2–5]

Although controversy regarding the mechanism of TBI still exists, recent studies have suggested that rotational, not linear head motion, is the primary cause of brain deformation, and leads to diffuse injuries ranging from mild concussion to diffuse axonal injury (DAI). This theory was originally hypothesized by Holbourn (in 1943) using fundamental mechanics to describe the motion of the brain relative to the skull.[6] The significance of axis-dependent rotational motion has been corroborated through numerous experimental[7–11] and computational studies.[3,4,12,13]

Finite element (FE) models have been vital to investigating TBI mechanisms, assessing injury risk and safety gear, and developing brain injury criteria based on external head kinematics. Various FE models of the head have been created to predict injury using strain-based injury metrics such as maximum principal strain (MPS) and the cumulative strain damage measurement (CSDM).[4,12,14] These models allow for the in-depth investigation of the brain response under various loading conditions at a level that is not possible using cadaveric or human experiments. Because brain strain is the primary outcome measure typically used to predict brain injury, it is essential to validate the brain deformation predicted by these models using human brain motion observed in laboratory experiments.

Various techniques have been utilized to study *in vivo*, *in situ*, and *in vitro* human brain motion in response to motion of the head.[15–17] One approach for investigating *in situ* brain motion has been high speed radiographic imaging of radio opaque objects implanted in the brains of postmortem human surrogates (PMHS). Stalnaker and colleagues[16] used lead markers to quantify brain

Center for Applied Biomechanics, University of Virginia, Charlottesville, Virginia.

Downloaded by Univ Of Western Ontario from www.liebertpub.com at 04/11/18. For personal use only.

motion during the repressurization of the vasculature and ventricles. Nusholtz and colleagues[18] injected a neutral-density radio opaque gel into the brain to measure brain motion in PMHS using high-speed cineradiography. Frontal impacts using a padded linear impactor on the specimen resulted in head linear accelerations ranging from 25 to 450*g*, head rotational velocities ranging from 18 to 52 rad/sec, and durations ranging from 8 to 50 ms. During these tests, minimal brain distortion was observed, except for displacements of 6 mm in a specimen that also sustained skull fracture.

Hardy and colleagues[15,19] used high-speed biplanar radiography to track the three-dimensional (3D) motion of neutrally dense targets (NDT), made from tin granulas embedded in polystyrene tubing, implanted in columnar and cluster arrays in the brains of PMHS head-neck specimens. The head-neck specimens were inverted and subjected to frontal, occipital, and coronal impacts. Impacts were imparted on the head using a padded linear impactor, which resulted in head linear accelerations ranging from 38 to 291*g*, rotational velocities ranging from 4 to 30 rad/sec, and head rotational accelerations ranging from 2370 to 24,206 rad/sec^2. The markers in the brain were observed to follow figure-eight patterns with peak to peak excursions as high as 13.4 mm. The results obtained from this study provided a valuable validation data set for FE model development, but included several limitations. Bi-planar radiography requires that each implanted NDT be continuously viewable in each frame, and each must be consistently distinguishable and identifiable from the other surrounding NDTs. This limits the number of NDTs that may be used in a given test, as too high of a concentration of markers in any area would confound distinct, consistent identification of the NDTs.[19] This continuous viewing requirement also limits the pattern of NDT placement that may be used. Targets cannot be placed in overlapping visual planes (i.e., at multiple depths), as this would result in visual interference of the NDT sets, restricting the placement of NDTs to planar columns or regional clusters. These limitations also required that different NDT patterns be used for tests in different rotation axes, meaning that most instrumented heads could only be tested in one direction. As a result, the brain displacement mappings available from those tests are limited to relatively small regions of the brain, with the locations of those mapped regions inconsistent across test types. High speed radiography also has a discretization limitation in tracking the positions of the NDTs, providing an inherent error of 0.24 mm on all measurements.[15,20] The method also limits test fixture design to prevent interference with X-ray videos, and constrains loading conditions such that the head trajectory is confined within the field of view of the X-ray system.

Other imaging modalities have also been used to characterize brain motion. Mallory and colleagues[21] conducted low-severity sagittal head rotations (2 rad/sec, 120–140 rad/sec^2) on repressurized cadavers, and measured brain deformation using B-mode ultrasound at the surface of the dura. The study was useful in identifying relative motion between the brain and surrounding anatomical structures. Bayly and colleagues,[17] Feng and colleagues,[22] Sabet and colleagues,[23] and Knutsen and colleagues[24] used tagged MRI to quantify *in vivo* brain deformation in human volunteers during low-severity, repeated sagittal head accelerations (2–3*g*, 40 ms) and coronal rotations (300 rad/sec^2, 40 ms). These studies provided valuable information on *in vivo* brain deformation, but were limited to low-speed head motions.

Many of the limitations of the existing methodologies for measuring brain deformation can be remedied using sonomicrometry. Sonomicrometry utilizes an array of small, implantable piezoelectric crystals to dynamically measure distances between points in the tissue by recording ultrasound time of flight between crystal pairs. This is a proven technology that has been extensively used for various *in vivo* and *in situ* biomedical research applications for the last 30 years, and has largely replaced biplanar radiography as the method of choice for high-rate internal motion tracking in cardiac mechanics.[20,25–28]

In a study of direct comparisons, 3D digital sonomicrometry was shown to have a high degree of agreement with measures derived from a materials testing machine (displacement difference of 0.037 ± 0.0137 mm),[29] a KUKA robot (displacement difference of 0.04 ± 0.001 mm),[30] single-plane fluoroscopy (absolute difference of 1.06 ± 0.27 mm),[31] and biplanar radiography (absolute difference of 0.63 ± 0.46 mm).[32] The study comparing sonomicrometry to biplanar radiography found an order of magnitude improvement in displacement accuracy, with spatial resolutions of 0.024 mm for sonomicrometry versus 0.24 mm for high speed radiography.[15,20] Further, sonomicrometry crystals do not have line-of-sight imaging requirements, which allows for a larger array of crystals that can be distributed throughout all regions of the brain, and allows each specimen to be tested in multiple loading conditions and directions.

The objective of this study was to develop and test a methodology for the investigation of 3D brain deformation during pure rotational loading of the head. The first goal was to demonstrate sonomicrometry as a tool for quantifying brain deformation. The second aim was to devise a well-defined test method to measure *in situ* whole brain deformation. The contributions of this study will provide a novel framework for quantifying brain deformation for generating biofidelity targets for FE model development.

Methods

Specimen acquisition and information

All tissue donation, testing, and handling procedures were approved by the University of Virginia Institutional Review Board–Human Surrogate Use (IRB-HSU) Committee. Exclusion criteria for the acquisition of the specimens included any factors that could compromise the anatomy or material properties of the skull and/or brain tissue, and included diagnosed skull lesions or trauma, neurological disease, or neurological lesions. All specimens were also screened for bloodborne pathogens (HIV, hepatitis A and B). The donated PMHS for this pilot study was a fresh, never frozen, 53-year-old male head-neck specimen acquired 14 h postmortem. Cause of death was congestive heart failure. The specimen was disarticulated at the first thoracic vertebra by the tissue supplier.

Table 1. Specimen Anthropometry and Mass Measurements

Component	*Anthropometric measurement*	*Outcome*
Whole body	Stature	173 cm
	Mass	116 kg
	BMI	38.8
Skull	Circumference	510 mm
	Length (ant.–post.)	172 mm
	Breadth (lat.–med.)	144 mm
	Height (vertex–mentum)	240 mm
	Brow-to-occiput arc length	315 mm
Mass	Head-neck	7.785 kg
	Brain[a]	1.265 kg

[a]Brain mass measured post-test during specimen dissection.

BMI, body mass index; ant., anterior; post., posterior; lat., lateral; med., medial.

Pre-test radiographs of the specimen confirmed no abnormalities of the skull. Specimen anthropometry and mass measurements are shown in Table 1.

Specimen preparation

All instrumentation and hardware installation were performed relative to the head center of gravity (CG), which was estimated based on anatomical landmarks according to the protocol outlined by Robbins and coworkers.[33] First, the Frankfort plane was identified by marking a line between the inferior margin of the orbit and the notch above the tragus. Lateral CG markings were drawn 8 mm anterior to the tragus on the Frankfort plane and 25% of the distance vertically from the Frankfort plane to the vertex of the skull. A posterior CG marking was defined at the midpoint of the circumferential line connecting the lateral markings, parallel to the Frankfort plane. The local head coordinate system was then defined in accordance with the Society of Automotive Engineers (SAE) J211 standards with the origin located at the head CG (at the midpoint of the line connecting the left and right lateral CG markings). Following identification of the CG, the skull was denuded and secured to the head rotation fixture by plates that were attached to the superior, lateral, and posterior surfaces of the skull. A custom-built jig was designed to ensure that all fixation plates were orthogonal to each other and centered on the desired axes of rotation (through the CG). Three mounting pins were used to align the skull CG within the jig at each CG marking, and a combination of wood screws and Bondo resin (3M, St. Paul, MN) were used to rigidly couple the fixation plates to the skull.

Sonomicrometry crystals (Sonometrics Corporation, London, Ontario, Canada) were employed to quantify brain deformation in response to the dynamic rotation pulses. The crystals are capable of transmitting and/or receiving ultrasound pulses to calculate distance using the speed of sound of the tissue. With the inclusion of at least three crystal pairs, trilateration can be used to determine the three dimensional coordinates of each receiving crystal. Initial testing of the crystals was performed *in situ* using porcine brain tissue, to confirm that the crystals could be easily inserted, functioned properly, recorded accurate data, and caused no gross disruption of the brain tissue.

A total of 32 crystals were utilized in this study, with transmitting crystals affixed to the inner skull and receiving crystals inserted in the brain tissue. An array of 24 crystals was inserted into the brain using a stereotactic cannulation system. A guide plate was fixed to the posterior surface of the skull to aid in the drilling of the ports. To introduce a crystal, a needle was first inserted into the 4.6 mm cannula and both were pushed to the desired depth within the brain. A needle was included in the cannula to prevent any coring of brain tissue. The needle was then removed and a small rod was used to push the crystal down the length of the cannula. The cannula was slotted to facilitate the removal of the cannula from around the crystal wires. In cases in which more than one crystal was passed through a single port, the cannula was retracted to the next insertion depth and the procedure repeated for the subsequent crystals (Fig. 1). Once all crystals were inserted, the ports were sealed using cord grips (Sealcon, Centennial, CO). The crystals inserted into the brain parenchyma were 2 mm in diameter, and were barbed with thin pieces of monofilament wire to anchor the

Downloaded by Univ Of Western Ontario from www.liebertpub.com at 04/11/18. For personal use only.

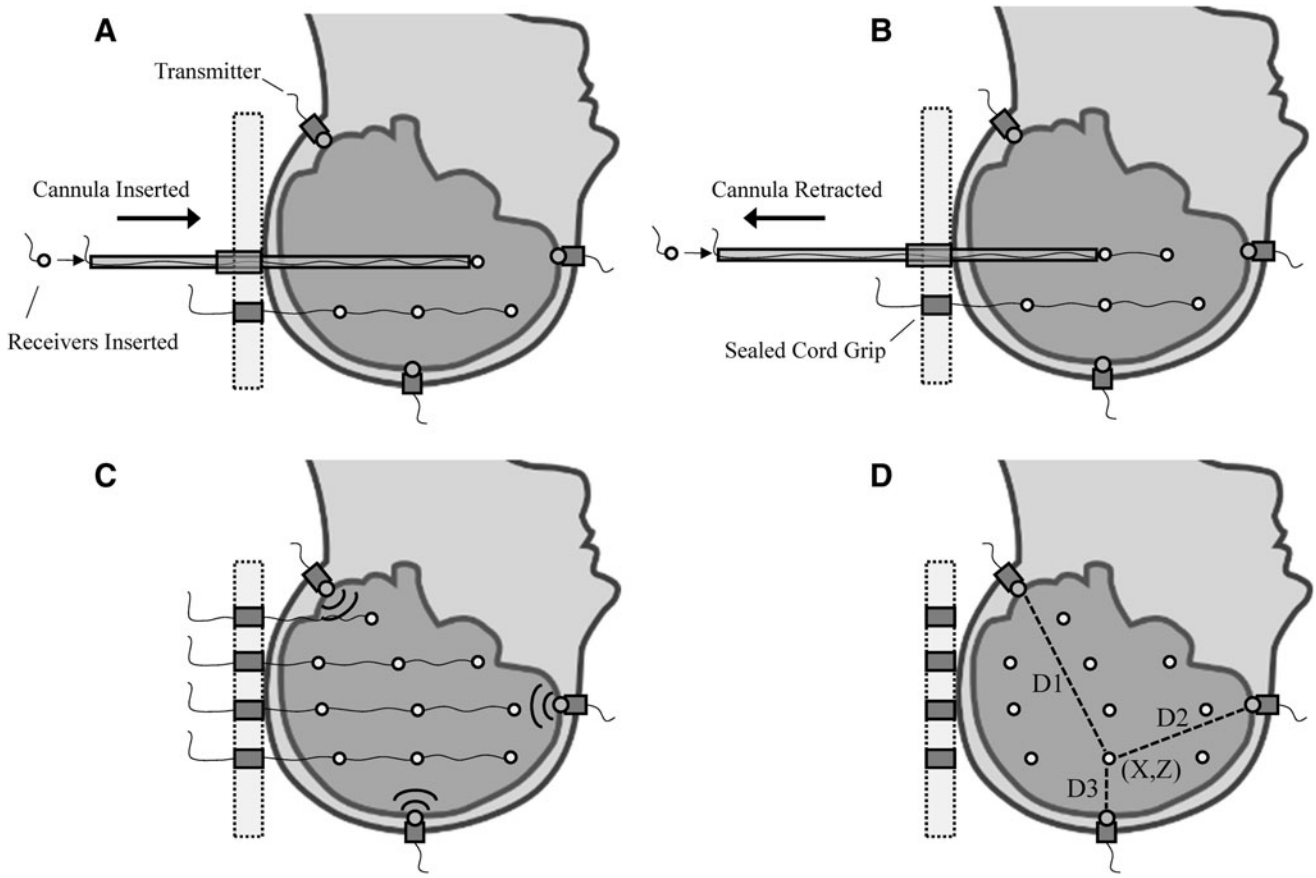

FIG. 1. Summary of crystal insertion procedure. **(A)** The cannula was inserted to the required depth and the crystal was pushed down the length using a rod. **(B)** The cannula was retracted and the next crystal was placed. The ports were sealed using cord grips. **(C)** During the test, the transmitters sequentially sent ultrasound pulses, while the receivers recorded the signals. **(D)** A minimum of three crystal pairs were necessary to find three-dimensional (3D) coordinates using trilateration.

Downloaded by Univ Of Western Ontario from www.liebertpub.com at 04/11/18. For personal use only.

crystals within the local brain tissue. Henceforth, all crystals inserted into the brain are designated as ''receivers,'' as their primary role was to act as passive receivers of the ultrasound pulses. The receiver array was designed to maximize the coverage of recorded brain deformation throughout the brain volume while avoiding the ventricles and the boundaries of the brain.

An array of 8 sonomicrometry crystals was fixed to the inner surface of the skull with a primary function of transmitting ultrasound pulses. Henceforth, these crystals will be referred to as ''transmitters.'' Larger 3 mm diameter crystals were used as transmitters for their increased transmission power. The position of the transmitter array was dictated by the maximum ultrasound transmission distance of the sonomicrometry crystals through the brain. Preliminary experiments using *in vitro* fresh porcine brain tissue determined this distance to be $\sim$100 mm. The transmitters were then fixed to the skull in locations that were determined to maximize transmission overlap throughout the brain. Following installation of the sonomicrometry instrumentation, CT images were acquired at a resolution of 0.625 mm, to determine the exact coordinates of each receiver and transmitter relative to the head CG.

Artificial cerebrospinal fluid (aCSF) was used to provide constant perfusion[34] throughout testing. The perfusion system applied a static pressure head of $\sim$78 mm Hg.[15] In addition to providing constant hydration and a consistent fluid boundary to the brain tissue, the perfusion eliminated any air pockets within the cranial cavity that could have interfered with ultrasound transmission. Perfusion was applied through vascular ports in the carotid arteries and transcranial ports located at the sagittal sinus and occiput. Fluid was allowed to drain through the jugular veins and the spinal cord. Perfusion fluid was constantly collected and recirculated to the static pressure reservoir during testing. Light perfusion was also applied during specimen preparation with refrigerated aCSF, to keep the specimen cool and hydrated to slow tissue degradation.

Test fixture and matrix

The target test condition was a pure rotation of the head around the head CG. A rotational test device (RTD) was designed to deliver repeatable and controlled rotations to the head about all three axes of rotation of the head (Fig. 2). The RTD was driven by a pneumatically driven linear actuator that was servo-hydraulically controlled with active feedback (DSD, Linz, Austria). The RTD used a cable-drive system to translate the linear output of the actuator into a rotational pulse. The drive drum was connected to a multi-directional bevel gear box to allow for applied rotations around the three axes of rotation of the head, while maintaining a consistent initial position of the head relative to gravity. In all cases, the head was inverted prior to the initiation of the test and returned to this position immediately following each test. For the sagittal and coronal pulses, the head fixture was mounted to the through-shaft of the gear box. For axial rotations, the head fixture was mounted to the perpendicular output shaft.

The test matrix included four haversine angular velocity pulses with calibrated maximum magnitude and duration. The pulses were chosen to represent a spectrum of severities relevant to automotive and sports impacts.[13] Four difference pulses were used, consisting of two rotational velocity magnitudes (20 rad/sec and 40 rad/sec) and two durations (30 and 60 ms). These were applied in each of the three rotation directions. A repeated test of the most severe loading case (40 rad/sec, 30 ms) was performed for each rotation direction, for a total of 15 tests on the same PMHS.

Instrumentation and data acquisition

Six degree-of-freedom (DOF) head kinematic measurements were acquired using a sensor array consisting of three Endevco 7264B-500 linear accelerometers (Meggit Sensing Systems, Irvine, CA) and three ARS PRO-8k angular rate sensors (Diversified Technical Systems Inc., Seal Beach, CA), which was rigidly mounted to the head. All data were transformed to the local head coordinate system as defined by SAE J211 standards.[35] A TDAS PRO data acquisition system (Diversified Technical Systems Inc., Seal Beach, CA) was used to acquire the data at a sampling rate of 10 kHz with an anti-aliasing filter of 2900 Hz. The linear acceleration data were filtered with a Channel Frequency Class (CFC) 1000 filter and the angular velocity were filtered with a CFC 60 filter. Angular acceleration was calculated by differentiating the filtered angular velocity data.

Sonomicrometry data was recorded using a 32 channel TRX-USB Acquisition System (Sonometrics Corporation, London, Ontario, Canada). Data were collected at a sampling rate of 560 Hz for the sagittal and coronal rotations, and at a rate of 709 Hz for the axial rotations. There were a total of 192 transmitter-receiver distance traces for each test. Before and after each test, static sonomicrometry data were collected to confirm that all receivers returned to their original position and that the crystals did not damage the brain tissue during testing or slip out of position.

Trilateration was utilized to determine the 3D coordinate time-history of each receiver crystal relative to the reference frame defined by the fixed transmitting crystals. This method uses the

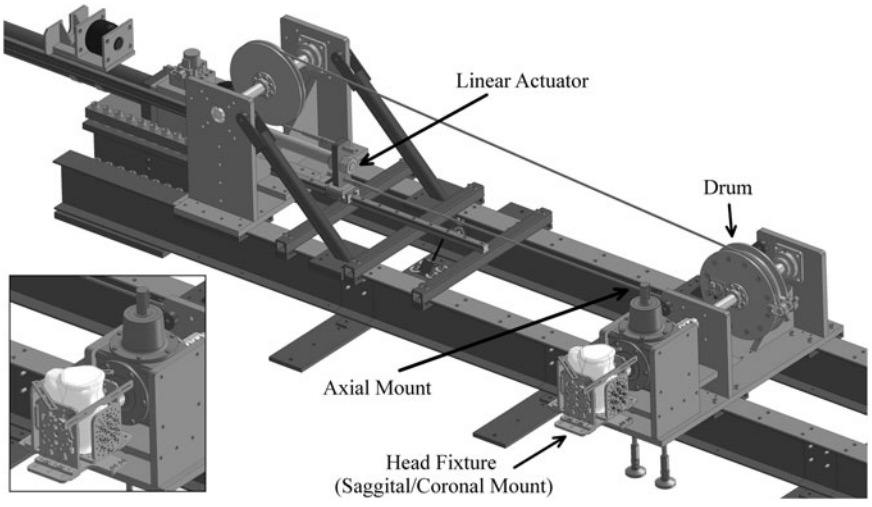

FIG. 2. Rotational test device with head fixture mounted.

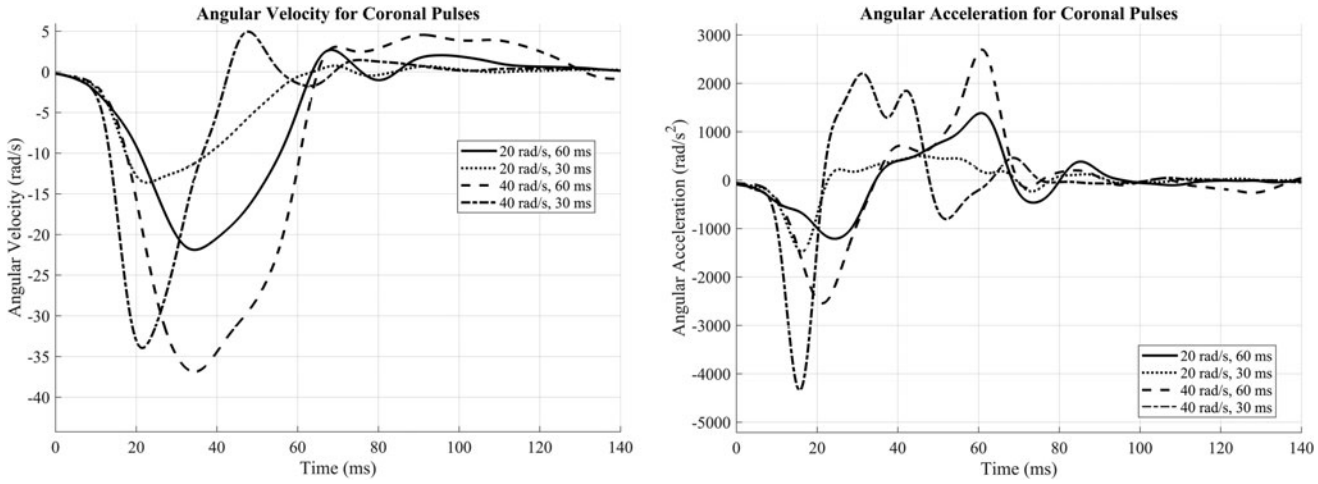

FIG. 3. Applied angular velocities and angular accelerations for all coronal tests.

Downloaded by Univ Of Western Ontario from www.liebertpub.com at 04/11/18. For personal use only.

geometry of spheres to determine the absolute location of a point based on multiple distance measurements. Trilateration calculations were performed using a multidimensional scaling algorithm to optimize the computed receiver coordinates based on the measured distances (SonoXYZ, Sonometrics Corporation, London, Ontario, Canada). The speed of sound was defined as 1550 m/sec for all computations. This value was found by optimizing the static sonomicrometry distances measured at the beginning of testing to those observed from CT images. This value is consistent with speed of sound values reported in the literature for brain tissue.[36,37] As sonomicrometry is inherently more accurate in capturing change in distance as opposed to absolute distance (errors of 24 μm in change of distance vs. 1.5 mm in absolute distance over a range of 10–120 mm), each distance trace was shifted so that the initial position of the trace matched the corresponding distance measured in the CT images. Following trilateration, all receiver coordinate time-histories were transformed to the head coordinate system.

Repeatability was assessed using a cross-correlation analysis tool (CORA)[38] which scores the similarity of two signals based on phase, shape, and magnitude (equally weighted). A perfect correlation (i.e., two equal signals) results in a score of 1. A root mean squared difference was also calculated for the repeatability of the applied head kinematics.

Results

All preparation and testing of the PMHS specimen was completed within 56 h postmortem. The static sonomicrometry data were used to calculate the difference in transmitter-receiver pair distances before and after every test to ensure that the crystals returned to their initial state following each test. On average, all crystal pairs returned to a position measuring 0.075 ± 0.032 mm of the pre-test distance. For brevity, the following results include data from only the coronal plane rotations. All other data and analyses will be presented in a future publication.

Head kinematics

There was minimal linear acceleration and off-axis rotation of the head for all loading severities. The angular velocity and angular acceleration traces for all coronal pulses are also shown in Figure 3. The average CORA score for the repeated tests was 0.93, with a standard deviation of 0.05. The root mean squared differences for those applied angular velocities was 1.3 rad/sec ±0.68 rad/sec for the 40 rad/sec (nominal) tests.

Sonomicrometry

The initial coordinates for each receiver and transmitter were obtained from the CT images and transformed to the head coordinate system following sonomicrometry instrumentation. During insertion, receivers 19, 21, 22, 26, and 32 were damaged and signals obtained from these receivers were unusable, yielding a total of 19 usable receivers. Figure 4 shows the positions of each receiver

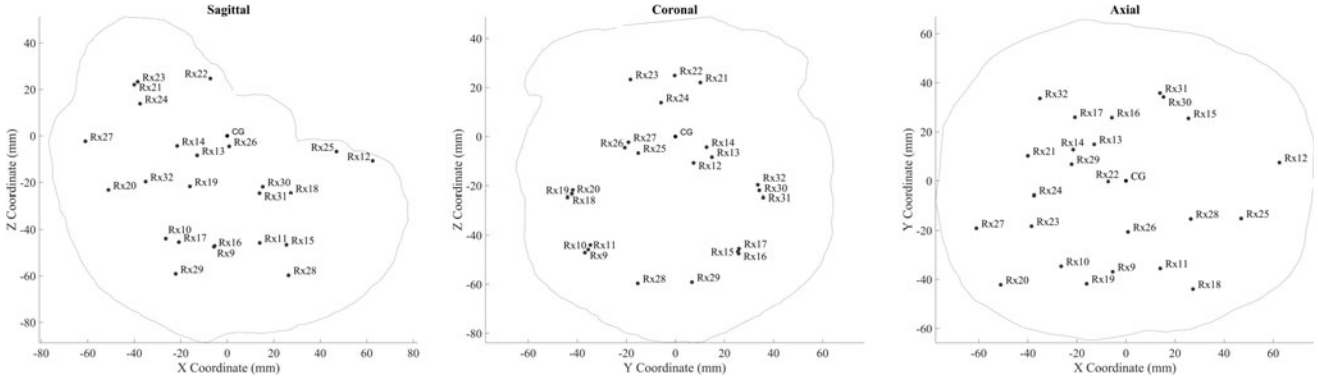

FIG. 4. Receiver positions projected to the sagittal (left), coronal (middle), and axial (right) planes. The head center of gravity (CG) position is indicated.

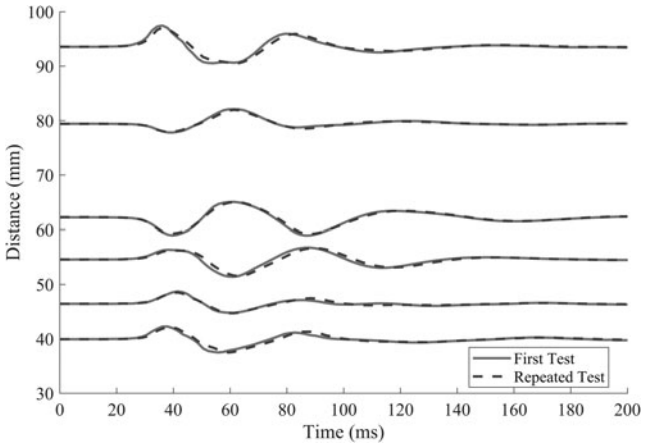

FIG. 5. Select distance traces for the repeated coronal 40 rad/sec, 30 m/sec pulses.

Downloaded by Univ Of Western Ontario from www.liebertpub.com at 04/11/18. For personal use only.

projected to the three anatomical planes. Select processed distance-time histories are shown for illustration in Figure 5 for the repeated coronal 40 rad/sec, 30 ms tests. The average CORA score for the repeatability of the crystal responses was 0.999 ± 0.001.

Trilateration was used to calculate the 3D displacement-time histories for each receiver. Trilaterated displacement plots for receivers 9, 16, and 13 in Figure 6 for each coronal test. Crystal trajectories in the coronal plane during each coronal test are shown in Figure 7. (Supplementary videos of receiver motion for the coronal—40 rad/sec—60 ms may be found at www.liebertpub.com/neu.)

Discussion

Finite element models of the brain are necessary for investigating brain mechanics during head motion. These models provide insight into brain injury mechanisms and also help establish brain injury risk functions. As such, it is imperative that the FE brain models are sufficiently validated for brain deformation using experimental data with well-defined boundary conditions and repeatable loading conditions that are consistent with those that cause TBI. In this study, a new methodology using sonomicrometry has been developed for quantifying dynamic, 3D brain deformation during rotational loading of the head. To our knowledge, this is the first published application of sonomicrometry in the brain and the first study to capture whole brain deformation fields caused by controlled, pure rotational loading in multiple directions using a human PMHS specimen. Although brain deformations at injurious levels have been quantified in the past using biplanar, radiography the method using sonomicrometry presents substantial improvements.

The primary disadvantage of biplanar radiography is the requirement for constant line of sight of the embedded NDTs. This has implications not only for mounting hardware and test fixture design, but also for the number and placement of the NDTs throughout the brain. As such, only a planar alignment or regional cluster of all NDTs can be used in biplanar radiographic tests, and specific NDT configurations are required for each direction of rotation or impact. Therefore, the utility of each specimen is limited. Sonomicrometry is capable of measuring brain deformation without these line-of-sight limitations. Provided that the sonomicrometry crystals can communicate with one another, a large number of them can be distributed in multiple, overlapping planes throughout the brain volume facilitating the mapping of 3D whole brain deformation. There is no line-of-sight limitation with the fixation hardware. The use of sonomicrometry does not impose constraints on the loading conditions and ensuing head trajectories, as long as there is enough slack in the crystal wires to remain plugged into the data acquisition system. The ability to test in all directions greatly increases the utility of each specimen, reducing the cost and time needed to obtain the 3D experimental data required to develop model validation targets. Further, sonomicrometry is an improvement on the spatial accuracy of the displacement measurements, and is not subject to limitations with camera resolution, image distortion, parallax, and errors encountered in coordinate system transformation.

In this study, a total of 15 tests in three directions were performed on a single specimen, spanning a range of angular velocities and durations. The rotational pulses applied to the head-neck specimen were informed by work done by Gabler and colleagues in 2017 that examined brain deformation from nearly 1000 reconstructed sled and crash tests using a human finite element brain model.[39] The reconstructed cases span a range of plausible head kinematics, from non-injury to concussion to moderate and severe TBI, based on injury criteria.[3,4,13,39,40] The Gabler study found that in most real-world impact environments, maximum brain deformation depends on the magnitude of angular velocity and angular acceleration (or rotation duration). From the deformation profiles, two peak angular velocities (20 and 40 rad/sec) and two impact durations (30 and 60 ms) were chosen to cover loading conditions observed in automotive and sports impacts associated with mild-to-moderate risk of injury.

Experiments seeking to produce reference data for FE model validation should use well-controlled, repeatable input conditions that are readily implementable in FE models. Results from inconsistent loading conditions (e.g., impactor tests in which the pulse is dependent on the mechanical behavior of the specimen) using multiple specimens cannot be readily combined into a common data set. In this study, the RTD was designed to apply pure, controlled, and repeatable rotational motion directly to the skull with the intent of comparing the biomechanics across different PMHS. An cross-correlation analysis of the repeat kinematic traces using CORA[38] found a score of 0.93 ± 0.05, showing excellent repeatability of the RTD input kinematics. A root mean squared difference across time for the repeated pulses in all directions yielded an average of 1.3 rad/sec ± 0.68 rad/sec for the 40 rad/sec tests. Although the motion was constrained to rotation in one direction, the system is a physical one with eccentricities, including the neck mass and an estimated axis of rotation of the head-neck specimen, which lead to off-axis loads and small linear accelerations. The off-axis rotations were found to be 3–12% of the maximum angular velocity in the primary loading directions (an average of 6.75%). Linear acceleration time-histories contained noise spikes reaching up to $100g$. However, because these linear accelerations occurred over small durations (1–2ms), when filtered at an appropriate frequency (300 Hz), the magnitude of linear accelerations was $<15g$ for all tests.

For all static data acquired before and after tests, the receivers returned to within 0.075 ± 0.032 mm of their original location. This result indicates two key findings. First, the sonomicrometry crystals did not slip relative to the surrounding tissue they were embedded in, and, therefore, were representative of the displacement of the surrounding tissue. Second, the loading conditions applied to the PMHS head, although at potentially injurious levels, did not result in gross structural damage to the parenchyma or supporting tissues.

Downloaded by Univ Of Western Ontario from www.liebertpub.com at 04/11/18. For personal use only.

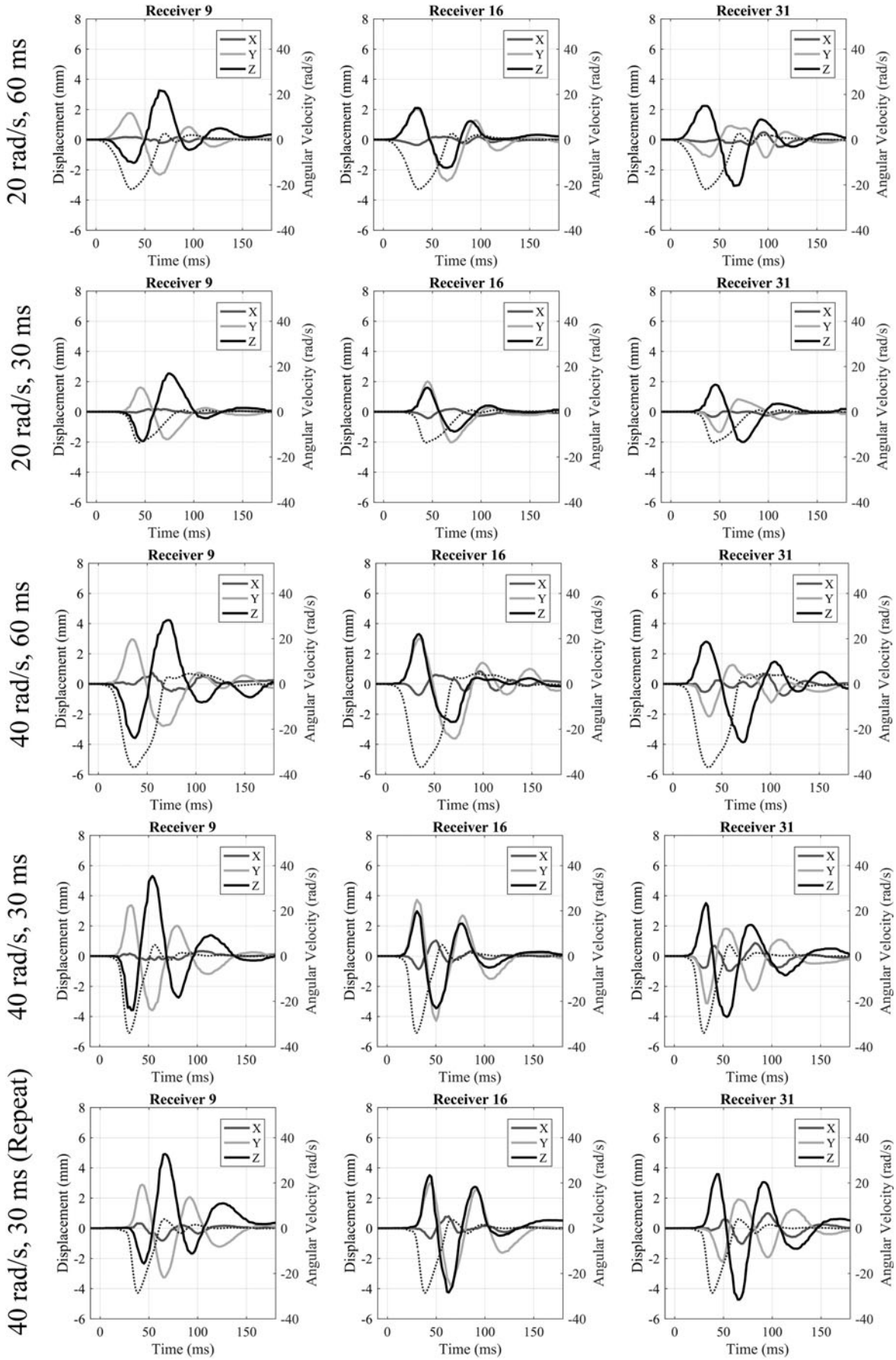

FIG. 6. Trilaterated displacement results for receivers 9, 16, and 31 for the coronal tests. The applied angular velocity pulse (dashed line) is overlaid.

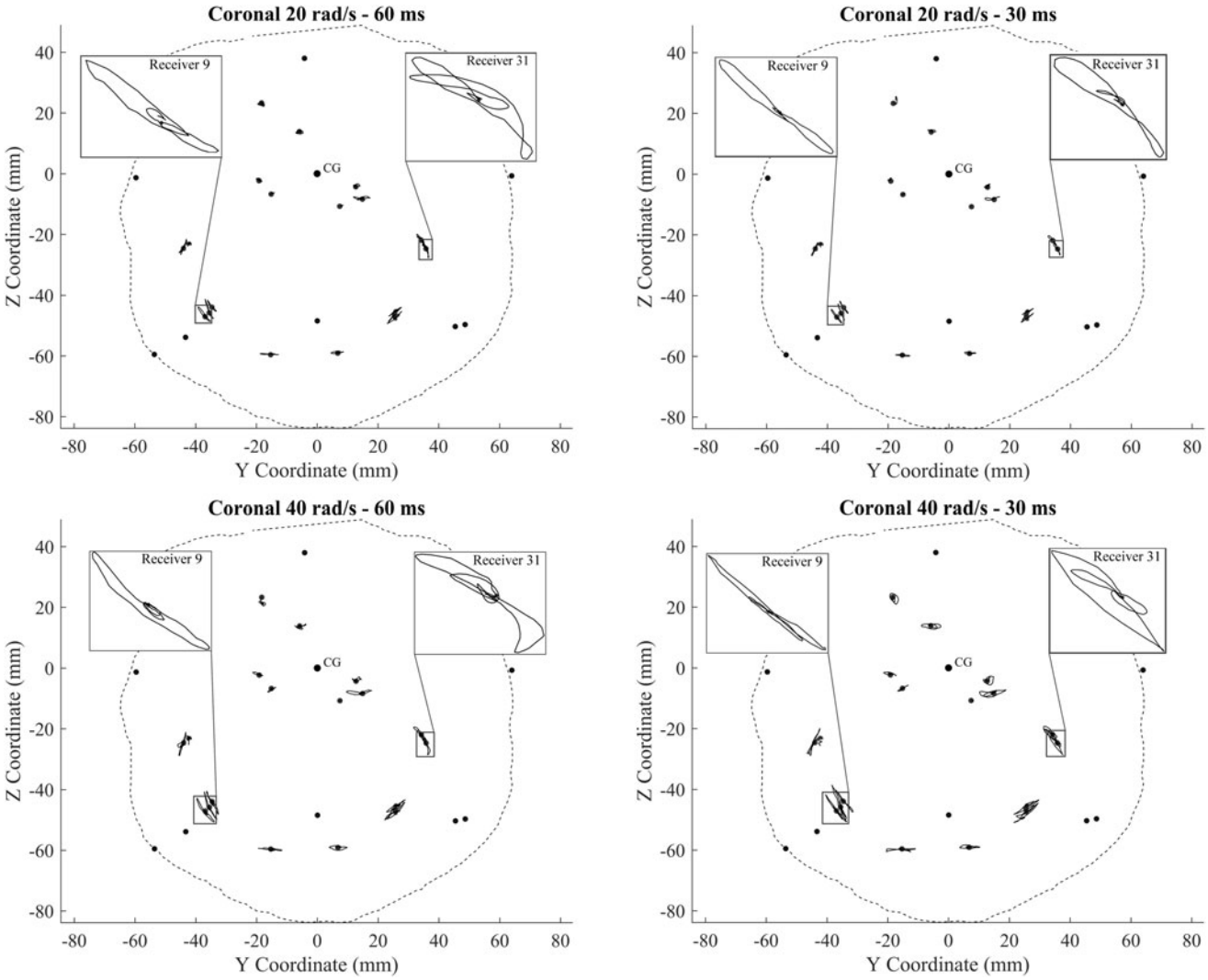

FIG. 7. Trilaterated receiver trajectories in the coronal plane for the coronal tests. Dots indicate the initial receiver and transmitter positions. A detailed view of receivers 9 and 31 is shown on the top.

Downloaded by Univ Of Western Ontario from www.liebertpub.com at 04/11/18. For personal use only.

This confirms that the cadaveric tissue integrity remained intact over the duration of testing, and that the techniques used to embed the crystals did not result in a loss of brain elasticity. It is important to clarify that the lack of structural damage does not necessarily mean that these loading conditions would not result in physiological brain injury in a living human. Mild TBI injuries typically present without observable physical damage or gross tissue disruption.[8]

The return of the crystals to their original position allowed for the testing of multiple rotation severities in all three planes. A second 40 rad/sec, 30 ms test was conducted for each axis of rotation to assess the repeatability of the proposed test conditions and sonomicrometry methods. Excellent repeatability, with an average CORA cross-correlation score of 0.999 ± 0.001, was observed in the distance measurements, and both sets of results were nearly identical in shape, phase, and magnitude (Fig. 5). This repeatability also translated to the trilaterated displacements and receiver trajectories (Fig. 6).

Trilateration was used to determine 3D displacement time histories for each receiver. Although the algorithm provided excellent results for most tests (Figs. 6 and 7), there were one or two cases in which the trilateration solution failed to converge properly despite the availability of good distance traces for that receiver. This was evident when the final trilaterated displacement did not return to its original position (~ 0 mm) despite that the individual distance traces between pairs of sensors returned to zero. These errors are likely indicative of a limitation in the trilateration algorithms utilized in the SonoXYZ software for this particular application of the sonomicrometry instrumentation. Future work should include developing a more robust algorithm for trilateration that is tailored for the sensor setup described in this study.

Three dimensional whole brain deformation data are critical for understanding the fundamental mechanical response of the brain. A diffuse array of crystals in the brain allows for the quantification of parameters describing the motion of individual crystals, such as peak-to-peak displacement, duration and frequency of the transient motion, and the lag time between the head and brain motions, as well as regionally dependent trends. The ability to test one head in all directions and loading severities also allows for comparisons of these parameters for the same crystals across head angular velocity magnitude, duration, and direction of head motion without preparation or specimen variability. For example, peak-to-peak displacements, defined as the maximum point-to-point displacement during the trajectory of each crystal, as large as 11, 12, and 23 mm were observed in the coronal, sagittal, and axial tests, respectively.

The transient response of the brain was observed to last between 100 and 200 ms after the initiation of rotation, suggesting a mechanical vulnerability of the brain during this time. The frequency response of the brain motion was found to be ~12–20 Hz, which is within the range of automotive crash and sports impacts to the head. The crystal trajectories typically formed an arcing path in the plane of rotation (Fig. 7). Although some regions experienced high deformations, others saw little to no motion of the brain crystals, which suggests that the brain deforms around an axis that is not coincident with the axis of rotation applied to the head. These observations suggest the potential for regions of vulnerability of the brain, which may be sensitive to direction, magnitude, and duration of loading.

Although Hardy and colleagues[15,19] were able to quantify brain deformation, it is difficult to conduct any comparison of the two data sets. The applied head kinematics in this study were purely rotational, whereas Hardy and colleagues conducted a series of impacts with resulting linear and rotational head kinematics. This study also utilized a single specimen to test all head directions, whereas Hardy and colleagues needed multiple specimens to test in different directions. The brain markers in the Hardy tests were at different locations compared with those in this study, and they were clustered within limited volumes of the brain. Additionally, the neck was constrained in the Hardy studies while the head was impacted, whereas this study allowed the neck to move with the head. A constrained boundary condition at the neck could potentially influence the deformation of the inferior regions of the brain caused by pulling through the cervical spine and spinal cord.

Conclusion

The availability of accurate, 3D deformation data of the human brain will help improve the biofidelity of FE brain models and will lead to better techniques for predicting and mitigating concussion risk. This study provides a novel, comprehensive methodology utilizing controlled mechanical input and sonomicrometry to measure 3D whole brain motion in dynamic head rotation tests. This methodology provides significant advantages over previous experiments, including:

- 3D motion capture of up to 24 sonomicrometry crystals within the brain without the need for biplanar radiography
- Ability to prepare and test a PMHS specimen rapidly postmortem, preserving tissue integrity
- Ability to test all three planes of rotation with no sensor adjustment, and minimal mechanical adjustments
- Repeatable, pure rotational inputs to vary the magnitude and duration of the head kinematics
- Repeatable brain motion measurements, as evidenced by the return of the crystals to their initial position and matching responses in the repeated test case.

Acknowledgments

This study was sponsored by the National Highway Traffic Safety Administration under contract number DTNH221500022/0002. The authors acknowledge the assistance and support of Kasia Rawska, Kevin Kong, Hongnan Lin, Kevin Kopp, Sara Heltzel, Ted Miller, Jim Bolton, Brian Overby, and Joey White.

References

1. Faul, M., Xu, L., Wald, M.M., and Coronado, V.G. (2010). *Traumatic Brain Injury in the United States.* Centers for Disease Control and Prevention National Center for Injury Prevention and Control: Atlanta.
2. Newman, J.A., Shewchenko, N., and Welbourne, E. (2000). A proposed new biomechanical head injury assessment function-the maximum power index. Stapp Car Crash J. 44, 215–247.
3. Rowson, S., and Duma, S.M. (2013). Brain injury prediction: assessing the combined probability of concussion using linear and rotational head acceleration. Ann. Biomed. Eng. 41, 873–882.
4. Takhounts, E.G., Craig, M.J., Moorhouse, K., McFadden, J., and Hasija, V. (2013). Development of brain injury criteria (BrIC). Stapp Car Crash J. 57, 243.
5. Versace, J. (1971). A review of the severity index. Society of Automotive Engineers (SAE) technical paper. No. 710881, pp. 771–796.
6. Holbourn, A.H.S. (1943). Mechanics of head injuries. Lancet 242, 438–441.
7. Ommaya, A.K., Grubb Jr, R.L., and Naumann, R.A. (1971). Coup and contre-coup injury: observations on the mechanics of visible brain injuries in the rhesus monkey. J. Neurosurg. 35, 503–516.
8. Gennarelli, T.A., Thibault, L.E., and Ommaya, A.K. (1972). Pathophysiologic responses to rotational and translational accelerations of the head. Society of Automotive Engineers (SAE) technical paper. No. 720970, pp. 296–308.
9. Gennarelli, T.A., Thibault, L.E., Tomei, G., Wiser, R., Graham, D., and Adams, J. (1987). Directional dependence of axonal brain injury due to centroidal and non-centroidal acceleration. Society of Automotive Engineers (SAE) technical paper. No. 872197, pp. 49–53.
10. Margulies, S.S., Thibault, L.E., and Gennarelli, T.A. (1990). Physical model simulations of brain injury in the primate. J. Biomech. 23, 823–836.
11. Smith, D.H., Chen, X., Xu, B.-N., McIntosh, T.K., Gennarelli, T.A., and Meaney, D.E. (1997). Characterization of diffuse axonal pathology and selective hippocampal damage following inertial brain trauma in the pig. J. Neuropathol. Exp. Neurol. 56, 822–834.
12. Kleiven, S. (2007). Predictors for traumatic brain injuries evaluated through accident reconstructions. Stapp Car Crash J. 51, 81.
13. Gabler, L.F., Crandall, J.R., and Panzer, M.B. (2016). Assessment of kinematic brain injury metrics for predicting strain responses in diverse automotive impact conditions. Ann. Biomed. Eng. 44, 3705–3718.
14. Zhang, L., Yang, K.H., and King, A.I. (2004). A proposed injury threshold for mild traumatic brain injury. Trans.-Am. Soc. Mech. Eng. J. Biomech. Eng. 126, 226–236.
15. Hardy, W.N., Foster, C.D., Mason, M.J., Yang, K.H., King, A.I., and Tashman, S. (2001). Investigation of head injury mechanisms using neutral density technology and high-speed biplanar X-ray. Stapp Car Crash J. 45, 337–368.
16. Stalnaker, R.L., Melvin, J.W., Nusholtz, G.S., Alem, N.M., and Benson, J.B. (1977). Head impact response. Society of Automotive Engineers (SAE) technical paper. No. 770921, pp. 303–335.
17. Bayly, P.V., Cohen, T.S., Leister, E.P., Ajo, D., Leuthardt, E.C., and Genin, G.M. (2005). Deformation of the human brain induced by mild acceleration. J. Neurotrauma 22, 845–856.
18. Nusholtz, G.S., Lux, P., Kaiker, P., and Janicki, M.A. (1984). Head impact response—Skull deformation and angular accelerations. Society of Automotive Engineers (SAE) technical paper. No. 841657, pp. 41–74.
19. Hardy, W.N., Mason, M.J., Foster, C.D., Shah, C.S., Kopacz, J.M., Yang, K.H., King, A.I., Bishop, J., Bey, M., Anderst, W., and others. (2007). A study of the response of the human cadaver head to impact. Stapp Car Crash J. 51, 17.
20. Dione, D., Shi, P., Smith, W., DeMan, P., Soares, J., Duncan, J., and Sinusas, A. (1997). Three-dimensional regional left ventricular deformation from digital sonomicrometry, in: *Engineering in Medicine and Biology Society, 1997. Proceedings of the 19th Annual International Conference of the IEEE.* IEEE, Chicago, IL, pps. 848–851.
21. Mallory, A.E. (2014). Measurement of Meningeal Motion Using B-Mode Ultrasound as a Step Toward Understanding the Mechanism of Subdural Hematoma. Doctoral Dissertation. The Ohio State University. Retrieved from ProQuest Dissertations Publishing.
22. Feng, Y., Abney, T.M., Okamoto, R.J., Pless, R.B., Genin, G.M., and Bayly, P.V. (2010). Relative brain displacement and deformation during constrained mild frontal head impact. J. R. Soc. Interface 7, 1677–1688.
23. Sabet, A.A., Christoforou, E., Zatlin, B., Genin, G.M., and Bayly, P.V. (2008). Deformation of the human brain induced by mild angular head acceleration. J. Biomech. 41, 307–315.
24. Knutsen, A.K., Magrath, E., McEntee, J.E., Xing, F., Prince, J.L., Bayly, P.V., Butman, J.A., and Pham, D.L. (2014). Improved mea-

Downloaded by Univ Of Western Ontario from www.liebertpub.com at 04/11/18. For personal use only.

surement of brain deformation during mild head acceleration using a novel tagged MRI sequence. J. Biomech. 47, 3475–3481.
25. Van Trigt, P., Bauer, B.J., Olsen, C.O., Rankin, J.S., and Wechsler, A.S. (1981). An improved transducer for measurement of cardiac dimensions with sonomicrometry. Am. J. Physiol. Heart Circ. Physiol. 240, H664–H668.
26. Sarazan, R.D., and Schweitz, K.T. (2009). Standing on the shoulders of giants: Dean Franklin and his remarkable contributions to physiological measurements in animals. Adv. Physiol. Educ. 33, 144–156.
27. Fomovsky, G.M., Rouillard, A.D., and Holmes, J.W. (2012). Regional mechanics determine collagen fiber structure in healing myocardial infarcts. J. Mol. Cell. Cardiol. 52, 1083–1090.
28. Holmes, J.W. (2004). Candidate mechanical stimuli for hypertrophy during volume overload. J. Appl. Physiol. 97, 1453–1460.
29. Stonecash, R.M. (2005). Evaluation of a Sonomicrometry System for the Measurement of Joint Kinematics. Doctoral Dissertation. University of Cincinnati. Retrieved from https://etd.ohiolink.edu
30. Sipes, N.S., Shearn, J.T., and Butler, D.L. (2005). Evaluation of a Sonomicrometry device for measuring in vivo dynamic joint kinematics: applications to functional tissue engineering. J. Biomech. 38, 2486–2490.
31. Meyer, S.A., and Wolf, P.D. (1997). Application of sonomicrometry and multidimensional scaling to cardiac catheter tracking. IEEE Trans. Biomed. Eng. 44, 1061–1067.
32. Meoli, D., Mazhari, R., Dione, D., Omens, J., McCulloch, A., and Sinusas, A. (1998). Three-dimensional digital sonomicrometry: comparison with biplane radiography, in: *Proceedings of the IEEE 24th Annual Northeast Bioengineering Conference*, Hershey, PA. pp. 64–67.
33. Robbins, D.H., Schneider, L.W., Snyder, R.G., Pflug, M., and Haffner, M. (1983). Seated posture of vehicle occupants. In: *Proceedings of the 32nd Stapp Car Crash Conference*. Paper No. 831617, pp. 199–224.
34. Sugawara, O., Atsuta, Y., Iwahara, T., Muramoto, T., Watakabe, M., and Takemitsu, Y. (1996). The effects of mechanical compression and hypoxia on nerve root and dorsal root ganglia: an analysis of ectopic firing using an in vitro model. Spine 21, 2089–2094.
35. SAE. (1995). *Instrumentation for Impact Test, Part I: Electronic Instrumentation*. SAE Paper No. J211/1. Warrendale, PA. Society of Automotive Engineers.
36. Azhari, H. (2010). Appendix A: typical acoustic properties of tissues. Basics Biomed. Ultrasound Eng. 313–314. John Wiley & Sons, Hoboken, NJ.
37. Kremkau, F.W., Barnes, R.W., and McGraw, C.P. (1981). Ultrasonic attenuation and propagation speed in normal human brain. J. Acoust. Soc. Am. 70, 29–38.
38. Gehre, C., Gades, H., and Wernicke, P. (2009). Objective rating of signals using test and simulation responses, in: *Proceedings of the 21st International Technical Conference on the Enhanced Safety of Vehicles, Stuttgart, Germany*. Paper 09-0407.
39. Gabler, L.F., Joodaki, H., Crandall, J.R., and Panzer, M.B. (2017). Development of a single-degree-of-freedom mechanical model for predicting strain-based brain injury responses. J. Biomech. Eng. [Epub ahead of print.]
40. Sanchez, E.J., Gabler, L.F., McGhee, J.S., Olszko, A.V., Chancey, V.C., Crandall, J., and Panzer, M.B. (2017). Evaluation of head and brain injury risk functions using sub-injurious human volunteer data. J. Neurotrauma.

Address correspondence to:
Matthew B. Panzer, PhD
University of Virginia Center for Applied Biomechanics
4040 Lewis and Clark Drive
Charlottesville, VA 22911

E-mail: mbp2q@virginia.edu

Downloaded by Univ Of Western Ontario from www.liebertpub.com at 04/11/18. For personal use only.